Polymer induced condensation of DNA supercoils

José Ésio Ramos, João Ruggiero Neto, and Renko de Vries

Citation: J. Chem. Phys. **129**, 185102 (2008); doi: 10.1063/1.2998521
View online: http://dx.doi.org/10.1063/1.2998521
View Table of Contents: http://jcp.aip.org/resource/1/JCPSA6/v129/i18
Published by the AIP Publishing LLC.

Polymer induced condensation of DNA supercoils

José Ésio Bessa Ramos, Jr.,[1] João Ruggiero Neto,[1] and Renko de Vries[2,a)]
[1]*Department of Physics, IBILCE UNESP, Universidade Estadual Paulista, R. Cristóvão Colombo 2265, 15054-000 São José do Rio Preto SP, Brazil*
[2]*Laboratory of Physical Chemistry and Colloid Science, Wageningen University, P.O. Box 8038, 6700EK Wageningen, Netherlands*

(Received 20 May 2008; accepted 18 September 2008; published online 10 November 2008)

Macromolecular crowding is thought to be a significant factor driving DNA condensation in prokaryotic cells. Whereas DNA in prokaryotes is supercoiled, studies on crowding-induced DNA condensation have so far focused on linear DNA. Here we compare DNA condensation by poly(ethylene oxide) for supercoiled and linearized pUC18 plasmid DNA. It is found that supercoiling has only a limited influence on the critical amount of PEO needed to condense plasmid DNA. In order to pack DNA supercoils in condensates, it seems inevitable that they must be deformed in one way or another, to facilitate dense packing of DNA. Analytical estimates and Monte Carlo simulations indicate that packing of DNA supercoils in condensates is most likely facilitated by a decrease of the superhelical diameter rather than by unwinding of the supercoils.
 [DOI: 10.1063/1.2998521]

I. INTRODUCTION

Ever since its discovery by Lerman,[1] crowding-induced DNA condensation has been intensively studied as a model for DNA condensation in living cells, especially bacteria.[2,3] The physical mechanism behind crowding-induced DNA condensation is the general mechanism for phase separation in mixtures of asymmetric colloids: depletion interactions between the solution components.[4] In model studies the crowding agent usually is a flexible polymer [such as poly(ethylene oxide) or PEO] that is supposed to mimic high intracellular concentrations of globular proteins that do not bind to DNA. Recent experimental studies have focused on studying crowding-induced DNA condensation at the single-molecule level[5] and on re-entrant decondensation at low polymer molecular weight.[6] Recent theoretical studies have elucidated the strong ionic-strength dependence of the condensation treshold[7] and have shown that nonbinding globular proteins are, in fact, much poorer DNA-condensation agents than flexible polymers,[8,9] consistent with experimental observations.[10] Whereas DNA in these studies is invariable assumed to be linear, DNA in bacteria is typically circularly closed and supercoiled due to the twist introduced into the DNA by both specific enzymes and by processes such as transcription and replication.[11]

Supercoiled DNA inside prokaryotic nucleids is condensed to such an extent that it is not unreasonable to speculate that, in fact, it might exhibit liquid crystalline order,[3,12] and indeed there is some experimental evidence pointing in this direction.[13]

In contrast to the large number of studies on liquid-crystallinity of linear DNA,[14] only a few experimental papers have addressed the arrangement of supercoiled DNA in liquid crystalline condensed states.[15–17] These studies do suggest that the structure of individual plectonemic supercoils changes upon condensation. However, with the scattering methods used in these papers, it is difficult to separate scattering due to intersupercoil and intrasupercoil interferences. For this reason, scattering experiments provide only limited information on the conformational changes of individual DNA supercoils in the presence of a high concentration of surrounding DNA supercoils. Analytical estimates by Odijk[12] suggest that condensation and liquid-crystalline ordering could ultimately lead to supercoil unwinding but only in very strong nematic fields. Some earlier theoretical work[18] has addressed the issue how DNA topology influences the shape and packing of DNA in the toruslike condensates that form at very low DNA concentrations.

In this paper, we study how supercoiling affects crowding-induced DNA condensation, by comparing polymer-induced condensation of supercoiled and linearized plasmid DNA. A simple condensation assay is used to determine the critical amount of polymer needed to condense the DNA molecules. We find that there is little difference between the critical amounts of polymer needed to condense linear and supercoiled plasmid DNA. Apparently, supercoiling does not introduce a large free energy penalty for packing DNA into condensates. Since the supercoils are quite large and the condensate densities quite high, this means that there are low-energy supercoil deformations that facilitate packing. To elucidate the nature of the possible low-energy supercoil deformations, we develop analytical estimates for supercoil unwinding and use Monte Carlo simulations of a single DNA supercoil, mimicking the dense environment of surrounding supercoils through the use of a nematic field and an effective depletion attraction between DNA segments.

a)Electronic mail: renko.devries@wur.nl.

II. MATERIALS AND METHODS

A. Plasmid DNA

The plasmid pUC 18 was extracted from *E. coli* using a Qiagen Plasmid Mega Kit. The linearized form was obtained by enzymatic digestion (2 h at 37 °C) of the supercoiled DNA using the restriction enzyme EcoRI. The DNA concentration was measured spectrophotometrally (1.0 OD at 260 nm equals 50 μg/ml. of DNA). The ratio between A_{260}/A_{280} was found to be equal to 1.88; the integrity of both forms was checked using agarose gel electrophoresis (1% agarose).

B. Condensation assay

The condensation assay was similar to that used by Murphy and Zimmerman.[10] PEO (molar mass 20 kg/mol) was dissolved in 30 mM tris-HCl, *p*H 7.0 After that, the NaCl concentration was adjusted to the required value using a concentrated NaCl stock solution. 50 μl solutions of PEO were prepared at given concentrations (measured in wt %) of PEO and NaCl. As the last component, we added pUC18 (linearized or supercoiled) plasmid DNA, again from a concentrated stock solution, to a final DNA concentrations of 12 μg/ml. Solutions were left at rest for 1 h and centrifuged for 1 h at 14 000 g, at room temperature. A small aliquot (5 μl or 10% of the total volume of the solution) of the supernatant was collected immediately after centrifugation and its DNA content was analyzed using agarose gel electrophoresis (1% agarose). Images of the gels were analyzed using IMAGEJ software.

C. Monte Carlo simulations

Monte Carlo simulations of DNA supercoils were carried out as described previously,[19] except that a Verlet neighbor list was used to speed up the evaluation of the nonbonded interaction energies. In brief, a single, circularly closed, DNA molecule was modeled as a closed string of N beads at positions $\mathbf{r}_1 \cdots \mathbf{r}_N$ (with $\mathbf{r}_{N+1}=\mathbf{r}_1$), interacting through a Hamiltonian H that includes terms for bond stretching, bending energy, twisting energy, nonbonded interactions between the beads, and a term ΔH mimicking the influence of an environment consisting of neighboring densely packed DNA supercoils:

$$H[\mathbf{r}_1, \ldots, \mathbf{r}_N] - \frac{1}{2}k_s\sum_{i=1}^{N}(|\mathbf{r}_{i+1}-\mathbf{r}_i|-l_b)^2 + \frac{1}{2}k_b\sum_{i=1}^{N}\arccos(\mathbf{t}_i\cdot\mathbf{t}_{i+1})^2 + \frac{2\pi^2 k_t}{N}(\Delta Lk - wr)^2 + \sum_{i=2,j<i}^{i=N} u(|\mathbf{r}_i-\mathbf{r}_j|) + \Delta H[\mathbf{r}_1, \ldots, \mathbf{r}_N]. \quad (1)$$

Unit tangents $\mathbf{t}_i$ are defined as $\mathbf{t}_i=(\mathbf{r}_{i+1}-\mathbf{r}_i)/|\mathbf{r}_{i+1}-\mathbf{r}_i|$, and k_s, k_b, and k_t are the elastic constants for, respectively, stretching, bending, and twisting. The equilibrium bond length for the beads is l_b, and ΔLk and wr are, respectively, the excess linking number and the writhe of the closed circular DNA. The isotropic potential of interaction $u(r)$ between the beads is taken to be a sum of steric repulsion and longer-ranged Debye–Hückel electrostatic repulsion,

$$\frac{u(r)}{kT} = \left(\frac{\sigma_d}{r}\right)^{12} + l_B\alpha^2\frac{\exp(-\kappa r)}{r}, \quad (2)$$

where σ_d is the DNA steric diameter, α is the strength of an effective Debye–Hückel point charge located in the center of the beads, $l_B=e^2/\varepsilon kT$ is the Bjerrum length, e is the elementary charge, ε is the solvent permittivity, and kT is the thermal energy. The Debye screening length of the electrostatic repulsion is $\kappa^{-1}=(8\pi l_B n_s)^{-1/2}$, where n_s is the number density of monovalent electrolyte.

The term ΔH is used to mimic the influence of an environment consisting of neighboring densely packed DNA supercoils on a single test DNA supercoil. We distinguish effective contributions at the one-segment and the two-segment level. At the one-segment level, the main effect is alignment and possible unwinding due to nematic ordering of surrounding DNA supercoils. This effect is taken into account through an effective nematic potential:

$$\Delta H_{\mathrm{nem}}[\mathbf{r}_1, \ldots, \mathbf{r}_N] = \frac{1}{2}k_n\sum_{i=1}^{N}(1-(t_i\cdot\mathbf{n})^2),$$

where k_n is the strength of the nematic field, and $\mathbf{n}$ is the nematic director. The two-segment level corresponds to effective interactions between the two segments of the test DNA supercoil induced by an environment of neighboring densely packed supercoils. At this level, we believe that the main effect is an effective depletion attractions between test segments in the presence of high concentrations of surrounding DNA segments (see Sec. III),

$$\Delta H_{\mathrm{depl}}[\mathbf{r}_1, \ldots, \mathbf{r}_N] = \sum_{i=2,j<i}^{N} u_{\mathrm{depl}}(|\mathbf{r}_i-\mathbf{r}_j|).$$

The functional form of the depletion potential between beads that we have used here is similar to that used in our previous work on depletion attractions between DNA segments in the presence of nonadsorbing globular proteins:[9]

$$u_{\mathrm{depl}}(r) = \begin{cases} v_{\mathrm{depl}}(1-r/\xi), & r \leqslant \xi \\ 0, & r > \xi \end{cases}$$

for some value of the strength v_{depl} and range ξ of the depletion interaction.

Trial moves consisted of small random translations of randomly chosen beads. Trial moves were accepted or rejected based on the Metropolis Monte Carlo criterium. The stepsize of the moves was adjusted to give an acceptance ratio of about 50%. Parameter values were the same as in Ref. 19, and correspond to DNA bend and twist persistence lengths of, respectively, 50 nm and 75 nm, and an ionic strength of 0.15M.

From the saved trajectories, we determine the values of the writhe and diameter of the supercoils. The writhe is computed from the full Gauss integral for the polygon.[20] For the effective supercoil diameter, we first determine, for each (test) bead, the distance to the closest neighboring bead, ex-

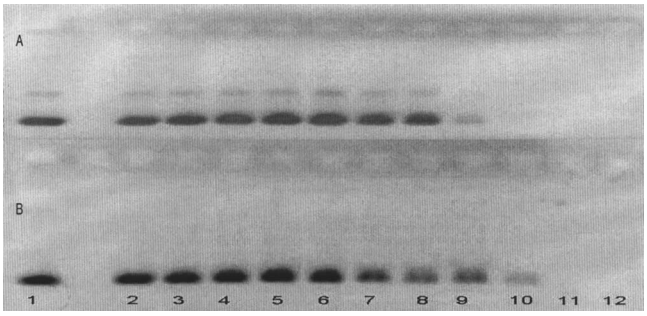

FIG. 1. Condensation assay. Mixtures with a fixed concentration of DNA and an increasing concentrations of PEO are centrifuged for 1 h at 14 000 g. The supernatant is analyzed with agarose gel electrophoresis. The figure shows typical gels for [NaCl]=0.15*M*. Lane 1: without PEO 20K; lanes 2–12: PEO 20K concentration increasing from 2 to 12 wt. %. (a) Supercoiled pUC 18, the faint band is a small amount of nicked DNA. (b) EcoRI linearized pUC18.

cluding 40 beads on the left and right sides of the test bead. The effective supercoil diameter reported is the average of these distances over all beads.

III. RESULTS AND DISCUSSION

A. Condensation assay

As can be seen in Fig. 1, the fraction of DNA in the supernatant after centrifugation starts decreasing at a PEO concentration close to 7% (w/v) at 0.15*M* of NaCl. Figure 2 shows the relative intensity of the bands for the supercoiled DNA and the corresponding linear form. As can be seen, the threshold concentration for condensation is nearly the same for both forms, the threshold for the supercoiled DNA being slightly higher than that of the linear DNA. Figure 3 shows the dependence of the critical PEO concentration as a function of the NaCl for both DNA topologies. The salt dependence is very similar for both DNA topologies, and is also very similar to the salt dependence that has been determined before for linear DNA using single-molecule fluorescence[5] and circular dichroism.[6]

B. Theoretical considerations

In previous theoretical work, we have shown that the critical concentration of flexible polymer needed to condense

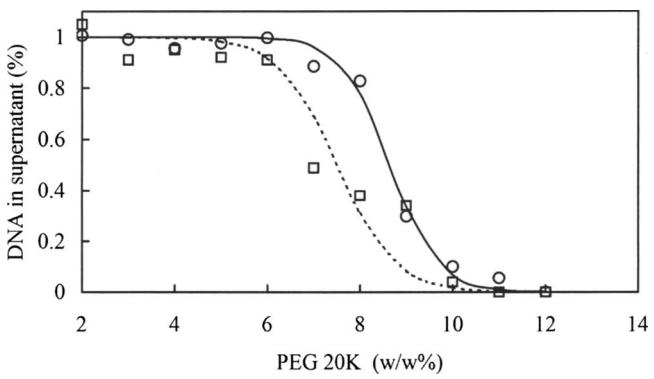

FIG. 2. Condensation assay. Intensity of the DNA bands as a function of wt % PEO 20K, again at [NaCl]=0.15*M*. Squares: EcoRI linearized pUC18. Circles: supercoiled pUC18.

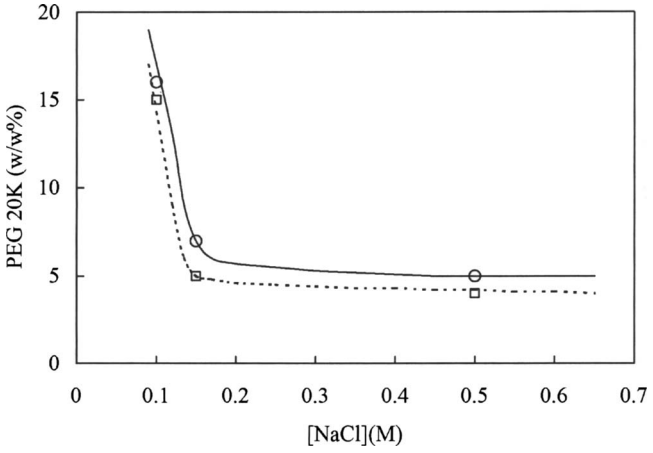

FIG. 3. Condensation treshold (PEO 20K wt % at which the intensity of the DNA bands in the condensation assay start decreasing) as a function of [NaCl]. Squares: EcoRI linearized pUC18. Circles: supercoiled pUC18.

DNA (assuming no flexible polymer is left in the condensates) can be estimated by equating the free energy of inserting DNA, respectively, in the free or condensed form in the polymer solution:

$$f_{\mathrm{ins,free}} = f_{\mathrm{ins,cond}}. \qquad (1')$$

Since generally the supercoil diameter is appreciably larger than the size or characteristic lengthscale of the crowding agent (in this case the correlation length of the semidilute PEO solution), the first term is expected to be essentially unaffected by DNA supercoiling, as was also argued previously by Odijk for the depletion of nonbinding globular proteins around supercoiled DNA.[3]

The second term $f_{\mathrm{ins,cond}}$ might be increased by supercoiling (leading to a higher boundary for condensation) if it costs more to pack supercoiled DNA to the same density as linear DNA. Packing problems may be alleviated by deformations of the supercoils. The absence of a strong effect of supercoiling on the amount of polymer needed to condense DNA suggests that the free energy associated with these deformations is small, most likely appreciably smaller than the packing free energy itself.

In this section, we estimate the deformation energy associated with supercoil unwinding and compare it to the estimated packing energy, in order to see whether supercoil unwinding can qualify as a low-energy deformation that could facilitate the packing of DNA supercoils in a condensate.

For a typical plasmid superhelical density of $\sigma=-0.06$, the twisting energy per unit length of DNA for the completely unwound configuration is

$$\frac{H_{\mathrm{twist}}}{L} = \frac{2\pi^2 CkT}{p^2}\sigma^2 \approx 0.4kT/\mathrm{nm}, \qquad (2')$$

where $p=3.4$ nm is the equilibrium DNA helical pitch, $C=75$ nm is the DNA twist persistence length, and L is the DNA contour length. The actual energy required to completely unwrithe the supercoil to a flat configuration (with writhe $wr=0$) is less than this, since not all excess linking is stored as writhe: typically $wr/\Delta Lk \approx 0.6$. Hence a somewhat

sharper upperbound for the energy of completely unwrithing the supercoil is

$$\frac{H_{\text{twist}}}{L} \approx 0.24kT/\text{nm}. \tag{3}$$

Partial unwrithing and decreasing the superhelical diameter should only cost a fraction of this. In order to compare this deformation free energy to the actual packing free energy of the supercoils, we assume the latter is rather close to the free energy of packing linear DNA to the same density. If this were not the case, we would certainly have seen larger differences in the critical amount of polymer needed to condense the DNA. The free energy f_{pack} (per unit length) of packing linear DNA into a condensate is estimated according to the theory of Odijk[21] for hexagonally packed gels of semiflexible polyelectrolytes:

$$\frac{f_{\text{ins}}}{kT} = \frac{3(2\pi)^{1/2}\xi_{\text{eff}}^2}{l_B}\frac{\exp\left(-\kappa D + \frac{1}{2}(\kappa u)^2\right)}{\left(1+\frac{1}{2}\kappa u^2/D\right)} + \frac{c_{\text{und}}}{u^{2/3}P}, \tag{4}$$

where D is the lattice spacing, u is the rms amplitude of the thermal undulations of the semiflexible chains, ξ_{eff} is the effective dimensionless linear charge density of DNA (computed as in our previous work), and the numerical constant is $c_{\text{und}}=2^{-2/3}$. For a given lattice spacing D, the undulation amplitude u is determined by balancing the electrostatic repulsion (the first term, which favors small values of u) against the configurational entropy (the second term, which favors large values of u). We assume some typical numbers: a DNA center-to-center distance in the condensates of $D=6.5$ nm, an ionic strength $c_s=0.15M$, which gives a dimensionless DNA charge parameter of $\xi_{\text{eff}}=7.0$, and an undulation amplitude $u\approx 0.9$ nm. Under these conditions, the osmotic pressure is $\Pi=4.3\times 10^4$ Pa, which corresponds to a PEO 20K concentration of about 7 wt %, close to the condensation threshold. For this case,

$$f_{\text{pack}} \approx 0.3kT/\text{nm}. \tag{5}$$

This is comparable to the free energy of completely unwinding the supercoils. Hence, significant unwinding is unlikely according to this estimate, since that would certainly lead to much higher packing energies and a higher boundary for condensation. Therefore, we should look for other low-energy deformations of the supercoils that could facilitate packing.

C. Monte Carlo simulations

Although we could also have developed estimates for other possible modes of deformation of DNA supercoils in condensates, such as a decrease of the superhelical radius, we instead decided to perform direct numerical simulations. Simulating a dense assembly of supercoils is at present too computationally intensive; therefore, we use a mean-field approach and simulate a single test supercoil under the influence of an averaged environment of surrounding supercoils. At the one-segment level, the main effect is nematic alignment, which has also been considered by Odijk.[12] We also consider the impact at the two-segment level: a dense environment of surrounding DNA supercoils will also influence interactions between two segments of the test supercoil.

1. Nematic fields

Following Odijk, we first consider the influence of a nematic field on configurations of plectonemic supercoils, where the nematic field is a simple approximation for the complex environment of nematic supercoils surrounding a certain test supercoil:

$$\Delta H_{\text{nem}}[\mathbf{r}(s)]/kT = \frac{1}{2}\Gamma P^{-1}\int_0^L ds[1-(\hat{\mathbf{n}}\cdot\hat{\mathbf{u}}(s))^2], \tag{6}$$

where $\hat{\mathbf{u}}(s)=\partial\mathbf{r}(s)/\partial s$ is the unit tangent along the continuous space curve $\mathbf{r}(s)$ describing the shape of the DNA of contour length L. The strength of the nematic coupling parameter Γ is related to the coupling strength k_n for the discrete DNA model used in the simulations by $\Gamma=k_nP/\langle l\rangle$, where $\langle l\rangle$ is the equilibrium bond length in the discrete DNA model (see Sec. II), and $P=50$ nm.

We simulated a small 1.3 kb DNA circle (corresponding to a contour length of about 450 nm) for two typical values of the superhelical density, $\sigma=-0.040$ and $\sigma=-0.055$, varying the strength of the nematic field from $\Gamma=0,\ldots,175$. For strong nematic fields, the orientational distribution is a Gaussian,

$$p(\theta) = \frac{\alpha}{4\pi}\exp\left(-\frac{1}{2}\alpha\theta^2\right), \tag{7}$$

where θ is the angle of the DNA axis with respect to the nematic director $\hat{\mathbf{n}}$. The constant α is related to the strength of the nematic potential by[12]

$$\Gamma = \tfrac{1}{4}\alpha^2. \tag{8}$$

From experimental data, Odijk[12] estimated that typically α does not increase much beyond O(10), implying that typically, $\Gamma<100$. Results for the superhelical diameter and the writhe from our simulations are shown in Fig. 4. At small field strengths, $\Gamma<30$, the supercoil responds by lowering its diameter. Only at very large field strengths, $\Gamma>30$, does the supercoil start unwinding (as shown by decreasing values of $wr/\Delta Lk$) at a relatively constant value of the superhelical diameter. Snapshots of typical configurations of the DNA supercoils without and with a (very strong) nematic field are shown in Fig. 5. The tentative upperbound of $\Gamma<100$ for DNA liquid crystals plus our simulation data indicate that a decrease of the superhelical diameter may certainly be expected, but that significant superhelical unwinding is unlikely consistent with the analyical estimates of the previous section and the estimates of Odijk.

2. Depletion attraction

The dense environment of supercoiled DNA not only tends to align individual DNA segments it also influences the effective interaction between two DNA segments of the test supercoil (for example, the interaction between segments on opposing sides of the plectonemic test supercoil). If we make a cut through the plane perpendicular to the nematic director, we have a two dimensional fluid of cross sections of DNA

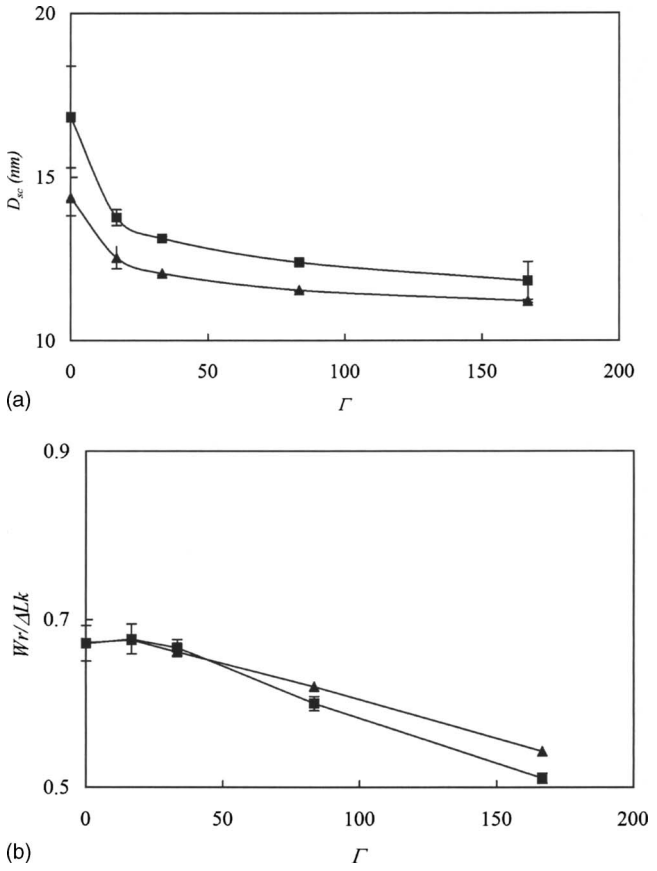

FIG. 4. Monte Carlo simulations of small 1.3 kb DNA circles in nematic fields, at two different superhelical densities: $\sigma=-0.040$ (squares) and $\sigma=-0.055$ (triangles). (a) Superhelical diameter D_{sc} as a function of the strength Γ of the nematic potential. (b) Writhe per added link $\mathrm{wr}/\Delta Lk$ as a function of the strength Γ of the nematic potential.

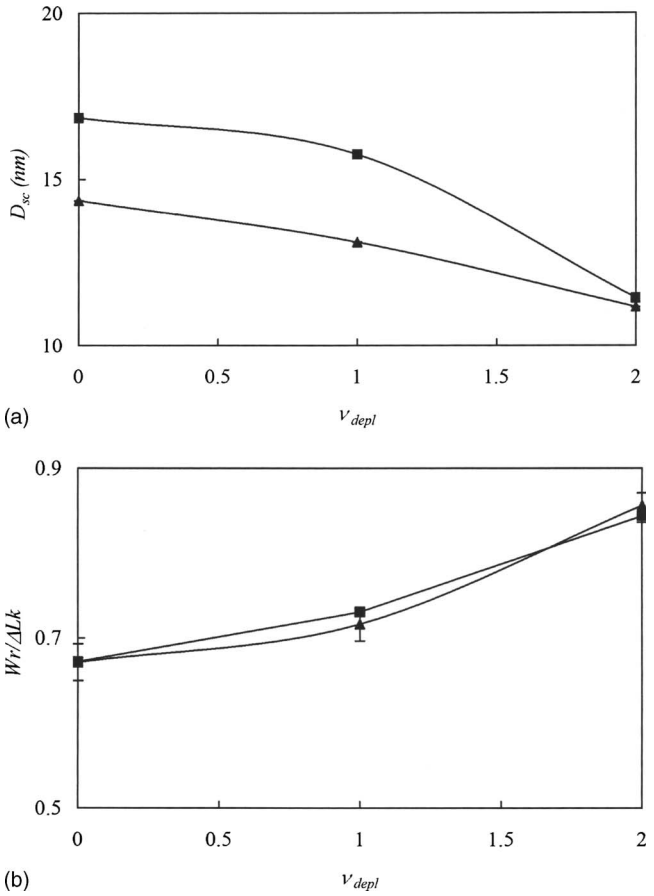

FIG. 6. Monte Carlo simulations of small 1.3 kb DNA circles with an added depletion attraction between the beads representing the DNA, at two different superhelical densities: $\sigma=-0.040$ (squares) and $\sigma=-0.055$ (triangles). (a) Superhelical diameter D_{sc} as a function of the strength v_{depl} of the depletion potential between the beads. (b) Writhe per added link $\mathrm{wr}/\Delta Lk$ as a function of v_{depl}.

segments with a pair-correlation function $g(r)$ that we can interpret in terms of a potential of mean force $u_{mf}(r)$ between two nearly parallel DNA test segments,

$$g(r) = \exp(-u_{mf}(r)/kT). \tag{9}$$

This potential of mean force $u_{mf}(r)$ has a contribution $V(r)$ due to the direct interaction between nearly parallel DNA segments and a contribution $\Delta V(r)$ due to the presence of the large number of DNA segments surrounding the two test segments,

$$u_{mf}(r) = V(r) + \Delta V(r). \tag{10}$$

The potential $\Delta V(r)$ is effectively a depletion attraction: for distances shorter than some characteristic exclusion length ξ,

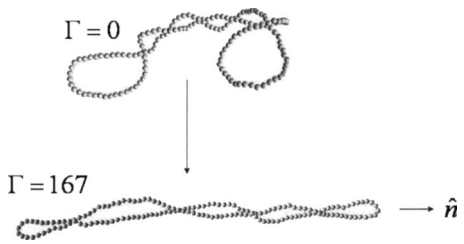

FIG. 5. Snapshot of typical configurations of the 1.3 kb DNA circles during the Monte Carlo simulations in the absence (top) and the presence (bottom) of a strong nematic field.

there will be no more DNA segment entering the space between the two test segments, and the test segments will be pushed together by the surrounding segments. For a crude estimate, we use the approach that we have previously used to estimate the depletion attraction between DNA segments (per unit length) induced by surrounding nonbinding globular proteins:[9]

$$\Delta V(r) \approx \begin{cases} -\frac{1}{2} f_{ins}(1 - r/\xi), & r < \xi \\ 0, & r > \xi \end{cases}, \tag{11}$$

where in the present case, f_{ins} is the free energy per unit length of inserting a test segment in the liquid-crystalline suspension of DNA supercoils (i.e., the DNA chemical potential per unit length),

$$f_{ins} \approx \Pi(D) D^2. \tag{12}$$

This corresponds to a strength v_{depl} of the depletion attraction per bead as used in the simulations of

$$v_{depl} \approx \Pi(D) D^2 \langle l \rangle = O(kT). \tag{13}$$

The exclusion range ξ is estimated as[9] $\xi \approx 2(\sigma_d + \kappa^{-1}) \approx 6.5$ nm. Figure 6 shows the results for the superhelical diameter D_{sc} and for the writhe $wr/\Delta Lk$ as a function of the strength of the depletion potential. Not surprisingly, the

depletion attraction decreases the superhelical diameter, with the largest changes being observed for the most loose supercoils, with superhelical density $\sigma=-0.040$. Perhaps more surprising is that the attraction opposes unwinding of the supercoils, because the attraction brings the configurations closer to that of the optimal plectonemic supercoil in which all twists are relaxed into writhe and which has a superhelical diameter that tends to zero. This should be compared to the predicted dependence of $wr/\Delta Lk$ and D_{sc} on ionic strength that is found in the absence of depletion attraction:[22–24] longer ranged repulsion then leads to a lower $wr/\Delta Lk$ and a higher D_{sc}. Thus, increasing the attraction changes $wr/\Delta Lk$ and D_{sc} in the same way as decreasing the electrostatic repulsion (by lowering the ionic strength).

IV. CONCLUDING REMARKS

We have shown that depletion condensation of DNA induced by flexible polymers is hardly hindered by DNA supercoiling. This suggests that packing of supercoils must be facilitated by supercoil deformations that cost very little free energy. In agreement with the scaling estimates, the simulations show that significant unwinding of supercoils in the condensates is not very likely: This only occurs in very strong nematic fields and is opposed by effective depletion attractions operating between DNA segments in the condensates. The lowest energy deformation, promoted by both a nematic field and by depletion attraction, is a decrease of the superhelical diameter. This therefore seems to be the most likely candidate for the deformation that is neccessary to pack DNA supercoils into condensates.

ACKNOWLEDGMENTS

We would like to thank Jan Verver and Joan Wellink for assistance with purifying and analyzing the DNA. E.B. was supported by a CAPES grant.

[1] L. S. Lerman, Proc. Natl. Acad. Sci. U.S.A. **68**, 1886 (1971).
[2] S. B. Zimmerman and L. D. Murphy, FEBS Lett. **390**, 245 (1996).
[3] T. Odijk, Biophys. Chem. **73**, 23 (1998).
[4] S. Asakura and F. Oosawa, J. Chem. Phys. **22**, 1255 (1954).
[5] V. V. Vasilevskaya, A. R. Khokhlov, Y. Matsuzawa, and K. Yoshikawa, J. Chem. Phys. **102**, 6595 (1995).
[6] J. E. B. Ramos, Jr., R. de Vries, and J. R. Neto, J. Phys. Chem. **109**, 23661 (2005).
[7] R. de Vries, Biophys. J. **80**, 1186 (2001).
[8] M. Castelnovo and W. M. Gelbart, Macromolecules **37**, 3510 (2004).
[9] R. de Vries, J. Chem. Phys. **125**, 014905 (2006).
[10] L. D. Murphy and S. B. Zimmerman, Biophys. Chem. **57**, 71 (1995).
[11] A. Bates and A. Maxwell, *DNA Topology*, 2nd edition (Oxford University Press, Oxford, 2005).
[12] T. Odijk, J. Chem. Phys. **105**, 1270 (1996).
[13] Z. Reich, Ellen J. Wachtel, and A. Minsky, Science **264**, 1460 (1994).
[14] F. Livolant and A. Leforestier, Prog. Polym. Sci. **21**, 1115 (1996).
[15] J. Torbet and E. Dicapua, EMBO J. **8**, 4351 (1989).
[16] Z. Reich, S. Levin-Zaidman, S. B. Gutman, T. Arad, and A. Minsky, Biochemistry **33**, 14177 (1994); S. Levin-Zaidman, Z. Reich, E. J. Wachtel, and A. Minsky, Biochemistry **35**, 2985 (1996).
[17] S. S. Zakharova, W. Jesse, C. Backendorf, and J. R. C. van der Maarel, Biophys. J. **83**, 1119 (2002).
[18] A. Yu. Grossberg and A. V. Zhestkov, J. Biomol. Struct. Dyn. **3**, 515 (1985).
[19] R. de Vries, J. Chem. Phys. **122**, 064905 (2005).
[20] K. Klenin and J. Langowski, Biopolymers **54**, 307 (2000).
[21] T. Odijk, Biophys. Chem. **46**, 69 (1993).
[22] A. Vologodskii and N. Cozarelli, Biopolymers **35**, 289 (1995).
[23] V. Rybenkov, A. V. Vologodskii, and N. R. Cozarelli, J. Mol. Biol. **267**, 299 (1997).
[24] J. Ubbink and T. Odijk, Biophys. J. **76**, 2502 (1999).